Digest Journal of Nanomaterials and Biostructures Vol. 10, No. 3, July - September 2015, p. 1087 - 1102

PREPARATION OF DISPERSED MONTMORILLONITE HOMOPOLYMER NANOGEL FOR REMOVAL OF WATER POLLUTANTS

A. M. ATTA[a,b*], H. A. AL-LOHEDAN[a], A. M. TAWFEEK[c],
A. A. ABDEL-KHALEK[d]
[a]*Surfactants research chair, chemistry department, college of science, King Saud university, Riyadh, KSA*
[b]*Petroleum Application department, Egyptian petroleum research institute, Cairo, Egypt*
[c]*College of science, king Saud university, Riyadh, KSA*
[d]*Chemistry department, Faculty of Science, Beni Suef University, Beni Suef, Egypt*

The present work used montmorillonite (Na-MMT) beside chemical crosslinker to prepare amphiphilic nanogel to increase their adsorption rate to remove water pollutants. In this respect, several ionic and nonionic monomers such as acrylic acid (AA), acrylamide (AAm), N-isopropylacrylamide, 2-acrylamido-2-methylpropane sulfonic acid (AMPS) and its sodium salt (AMPS-Na) are used to prepare homopolymer nanogels having different chemical structures. The chemical interactions between nanogels and Na-MMT and their chemical structure were confirmed by FTIR analysis. The intercalation and exfoliation of Na-MMT were confirmed by wide-angle X-ray diffraction. The morphology of Na-MMT nanogel composites was investigated by TEM analysis. he surface properties of the prepared nanogels were determined from water surface tension measurements of different concentrations of Na-MMT nanogels. The prepared Na-MMT nanogels were used to remove methylene blue dye, cobalt and nickel cations from water at different pH solutions. The data confirmed that the Na-MMT nanogels having ability to reduce the surface tension of water have strong ability to remove dye and metal ions from water.

(Received July 16, 2015; Accepted September 21, 2015)

Keywords: Clay; nanomaterials, water treatment; nanogels

1. Introduction

There are several treatments used to modify the clay minerals to enhance their performance for specific catalytic, industrial and environmental applications [1-5]. These treatments include ion exchange and crosslinking reactions are based on converting clay minerals to organophilic minerals by intercalation or exfoliation of silicate layers to improve their surface area to volume ratios [6-8]. Polymer/clay nanocomposites (PCNs) are special types of composites that included the reinforcement phase in the nanometer size [9]. There are several attempts increase growing in the production of PCNs in the last decades to use in environmental applications and water treatments [10-12]. PCNs showed dramatic improvement in physico-chemical characteristics of clay such as thermal, mechanical and barrier characteristics [13-15]. Moreover, they offer corrosion resistance and environmentally friendly green composites which promote their recycling and environmental impacts [16]. To achieve these goals, new approaches of clay modifications are used to commercialize the organic modified clay minerals. Recently, the nanogel composites based on silica, clay, titania and metal oxides attracted great attention for removal of organic and inorganic water pollutants [17-20].

The inorganic nanogel nano-polymer composites (INPCs) are now recognized as superior materials that exhibit unique properties that cannot obtained by blending or complixing the organic

*Corresponding author: aatta@ksu.edu.sa

and inorganic components [21]. The preparation of INPCs is based on preparation of colloidal inorganic noanogels followed by dispersion into crosslinked polymers using solution crosslinking radical polymerization methods [22-25]. However, the aggregation of inorganic particles into the polymer composite affected their performance [26]. The miniemulsion polymerization technique utilized this problem but this technique required specialist equipments [27]. Recently, poly (vinyl pyrrolidone) (PVP) and poyl(vinyl pyridines), p2-VP attracted great attention to solve the aggregation problems [28-30]. It was previously reported that, PVP is used to intercalate the silicate layer and to enhance the adsorption efficiency of PCNs [31-33]. In this respect the present work, PVP as dispersing agent using water and ethanol as solvent used to disperse montmorillonite (Na-MMT) to use as a physical cross-linker for the synthesis of amphiphilic nanogels. Herein we report full details of the synthesis and characterization of a series of colloidal nanocomposites homopolymer-clay using surfactant free technique to polymerize different types of vinyl monomers (Scheme 1). We present a novel route to based on preparing amphiphilic nanogels having ability to reduce water surface tension to increase the pollutant diffusion inside the nanogel networks. The solution properties of the nanogels were examined by drop shape analysis (DSA), and means of dynamic light scattering (DLS), and the chemical structure and morphology were determined by Fourier-transform infrared (FTIR) spectroscopy, X-ray diffraction (XRD), and transmittance electron microscopy (TEM) as well.

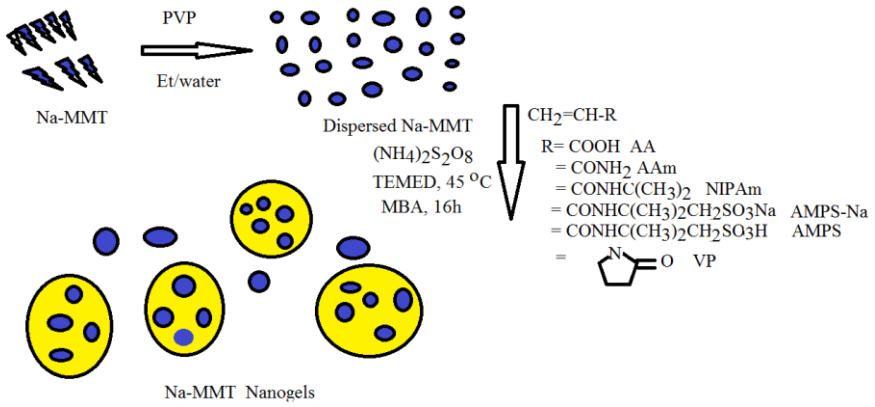

Scheme 1: Preparation of Na-MMT homopolymer nanogels

2. Experimental

2.1. Materials

The monomers acrylic acid (AA), acrylamide), N-isopropyl acrylamide (NIPAm), sodium 2- acrylamido-2-methylpropane sulfonate (Na-AMPS), and 2-acrylamido-2-methylpropane sulfonic acid (AMPS) are obtained from Aldrich Chemicals Co. and purified before using in the polymerization process to remove inhibitors. Sodium montmorillonite nanoclay (Na-MMT) with commercial name nanometer PGV is obtained from Sigma-Aldrich Co. Poly(vinyl pyrrolidone) (PVP) with molecular weight 40000 g/mol is used as dispersing agent for Na-MMT purchased from Aldrich Chemical Co. N,N-Methylenebisacrylamide (MBA), ammonium persulfate (APS) and N,N,N′,N′-tetramethylethylenediamine (TEMED) are used as crosslinker, radical initiator, and activator for crosslinking polymerization at low temperature, respectively and they purchased from Sigma-Aldrich Co. Deionized water and ethanol are analytical grades used as solvent for crosslinking polymerization. Methylene blue, cobalt and nickel nitrate hexa hydrate produced from Sigma-Aldrich CO. are used to prepare stock solutions of 100-1000 ppm. Buffer solution (H_3PO_4/NaH_2PO_4) was prepared by titration of 0.1 N of NaH_2PO_4 against 0.1 M HCl (for pH range 2 – 3) or against 0.1 N NaOH (for pH range 7 – 12) until the required pH is reached. The pH value was monitored using pH meter.

2.2. Synthesis procedure

Na-MMT clay was not easy to disperse in water solution. Therefore water/ethanol (60/40 vol %) mixture was used as solvent to disperse Na-MMT. In this respect, Na-MMT (2 g) is dispersed in water/ethanol (100 mL) and PVP (0.3 g) as stabilizer at room temperature for 24 hrs.

The dispersed Na-MMT nanogels based on NIPAm were prepared using surfactant free dispersion radical crosslinking polymerization using temperature programmed technique. In this respect, NIPAm monomer (0.5 g) is dispersed in Na-MMT solution (water/ethanol 50 mL). The solution was initially pre-heated at temperature 40 ° C under nitrogen atmosphere for 30 min. APS (0.015 g/ml) was added to start the polymerization. The reaction temperature was increased to 50 °C at rate 5 °C per 15 minute. The NIPAm monomer (1.5 g), MBA (0.03 g) and 20 µl TEMED were dispersed in the remained Na-MMT solution (water/ethanol 50 mL) and added dropwise to the reaction temperature during 1h. After 15 min, APS (0.02 g) dissolved in 2 ml of deionized water was injected into the reaction mixture. The reaction temperature was decreased to 45 ^{o}C to complete the stirring for 24 hrs. The dispersed Na-MMT/PNIPAm nanogel solution was centrifuged at 12000 rpm for 30 minute five times and washed with ethanol and dried under vacuum at 30 ^{o}C. The remained NIPAm (1.5 g) was mixed in Na-MMT dispersed aqueous solution (50 mL).

The same procedure was repeated to prepare Na-MMT nanogels with AA, AAm, VP, AMPS, AMPS-Na and AMPS. The prepared Na-MMT nanogels were washed with water, ethanol and acetone one time each, and the prepared particles were centrifuged (24680 rpm, at 20 °C) and then dried in an vacuum oven at 35 °C.

2.3. Characterization:

Fourier transform infrared (FTIR) spectrometer (Nicolet, NEXUS-670) used to determine the chemical structures of Na-MMt nanogels .

Wide-angle X-ray diffraction (WAX; Rigaku D/MAX-3C OD- 2988N X-ray diffractometer; CuKα radiation; λ= 0.15418 at 40 kV and 30 mA) is used to confirm the intercalation and exfoliation of Na-MMT galleries by nanogels.

Transmission Electron Microscope (TEM, JEOL JEM-2100 F) electron microscope and high resolution HR-TEM images recorded at an acceleration voltage of 200 kv are used to determine the nanogel morphologies.

Thermal stability and Na-MMT contents were determined using thermogravimetric analysis (TGA-50 SHIMADZU) at a heating rate of 10 ^{o}C /min.

Zeta potentials, particle size (nm) and particle size distribution index (PDI) of the modified Na-MMT nanogel were measured in aqueous solution in the presence of KCl (0.001 M) at different aqueous pH solutions using Laser Zeta meter Malvern Instruments Model Zetasizer 2000.

Double beam UV/vis spectrophotometer (model) was used to determine the absorbance of methylene blue dye (at 662 nm).

Atomic absorption spectroscopy (AAS; Perkin-Elmer 2380) was used to determine metal analysis in the direct aspiration into an air-acetylene flame.

The surface activity, surface tension in aqueous solution and interfacial tension between water and toluene are measured at 25 ^{o}C using drop shape analyzer model DSA-100.

2.4. Adsorption and desorption experiments

The adsorption kinetics of methylene blue onto Na-MMT nanogels was measured at different initial concentrations 100 and 1000 ppm of MB. In this respect, 50 ml of aqueous methylene blue solutions was introduced into a 100 ml conical flask under stirring in the presence of 0.01 g of the Na-MMT nanogels at 25 °C. The filtrate samples were analyzed at different time intervals after filtration. The concentration of MB in the residual solution was determined using

UV-Vis spectrophotometer at wavelength 662 nm. The amount of dye adsorption at equilibrium Q (mg/g) and percent extraction (%E) was calculated from the following equation:

$$Q= [(C_o-C_e) \times V/ (m)] \quad (1)$$

$$\%E= [(C_o-C_e) \times 100/(C_o)] \quad (2)$$

Where C_o and Ce (mg/L) are the liquid phase concentrations of dye at initial and equilibrium, respectively, V (L) the volume of the solution and m (g) is the mass of adsorbent used.
The same equations are used to calculate the adsorption of Co^{2+} and Ni^{2+} cations using AAS.

3. Results and discussion

Na-MMT is one of the most important clay minerals that have different applications in water treatments [34-36]. The ion exchange, adsorption of organic compounds and reactions with organic acid treatments are an effective methods used to replace sodium cations between silicate layers to intercalate the silicate layers and converting layers to organophilic minerals [37]. The crosslinking mechanism is another technique used to form dispersed Na-MMT composite [38]. In this respect, The scheme of encapsulation of Na-MMT using crosslinked nanogels based on homopolymers is represented in the scheme 1. The formation of Na-MMT nanocomposite has been achieved in dispersion polymerization, using PVP as stabilizer and H_2O/EtOH (solvent) as illustrated in the experimental section. The mechanism of crosslinking of homopolymers based on AA, AMPS, AMPS-Na, AAm, NIPAm and VP was carried out by using free radical polymerization in surfactant free medium. This technique produces functionalized Na-MMT amphiphile. AA, AMPS are acidic monomers used to study the ability of acidic monomers to coat basic Na-MMT. Moreover, AAm, NIPAm and VP are used as neutral monomers. AMPS-Na is ionized monomer selected to investigate the stability of Na-MMT colloids. The concentration of monomers plays important factor to produce stabilized Na-MMT nanogel colloids. The experiments confirmed that the presence of an stabilized hydrophilic Na-MMT in PVP and H_2O/EtOH at pH10, the crosslinking free radical polymerization of all monomers at 55 °C for 24 h led to a milky white dispersed Na-MMT polymer colloids, with no evidence of any macroscopic precipitation. Moreover, the crosslinking of monomers in absence of Na-MMT produced polymer precipitates without colloidal formation. This clearly demonstrates the crucial role played by the dispersed Na-MMT in producing colloidal stable dispersions based on core-shell technique as described in scheme 1. This mechanism was supported by previous data that indicated that the exfoliated clay platelets could be act as a kind of multifunctional physical cross-linking agent beside MBA crosslinker to form microgels [39].

3.1. Characterization of polymer-montomorillonite nanocomposite

The chemical structure of Na-MMT nanogels was elucidated with FTIR spectra illustrated in Fig. 1a-e. The characteristic bands at 526, 463 and1043 cm^{-1} (Si-O OH stretching of the silicate layers), 620 cm^{-1} (Al-O) and 1640, 3432, 3630 cm^{-1} (O-H OH stretching of the clay silicate layers) are used to confirm the Na-MMT chemical structure [40]. The new bands at 2950 and 2875 cm^{-1} (C-H stretching vibration of aliphatic) and disappearance of bands at 3100-3000 cm^{-1} (C-H stretching vibration of olefin) in the all spectra (Fig. 1a-e) confirm the polymerization and crosslinking of all monomers to form Na-MMT nanogels. The new bands at 1680 (CONH stretching) and 1540 cm $^{-1}$(NH stretching) indicated the presence of amide groups of MBA crosslinker and NIPAm, AAm, VP, AMPS-Na and AMPS polymers. The overlaps between Na-MMT band and polymers makes difficult to determine the interaction between Na-MMT layers and polymers. Accordingly, FTIR spectra (Fig.1 a-e) are used to confirm the formation of Na-MMT organiphilic after removal uncrosslinked polymers with washing several times with water.

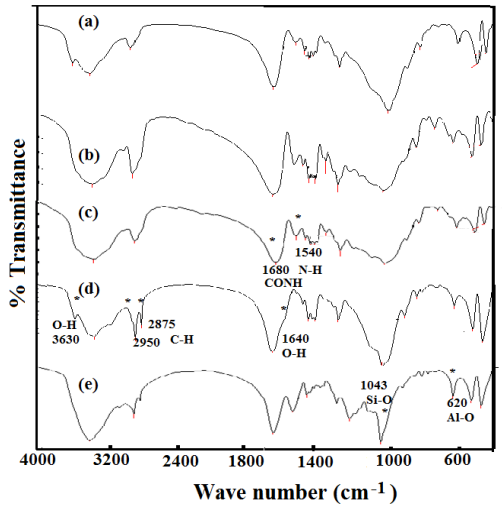

Fig.1. FTIR spectra of Na-MMT nanogels polymers a) PNIPAm, b)PVP, c)PAAm, d)PAMPS and e)PAMPS-Na

The amount of polymers used to intercalate or adsorbed at Na-MMT surfaces can be determined from TGA, DTG as illustrated in Fig.2 and tabulated in Table 1. The data of TGA indicates that Na-MMT included 5 (wt %) of water between sheet and loosed at 105 ^{o}C. The water contents was increased up to 8 to 12 wt % as polymer contents increased between Na-MMT galleries due to increment of their swelling characteristics with crosslinking between Na-MMT sheets. Careful inspection of data (Table 1) indicated that the polymer contents increased for Na-MMT coated with PNIPAm, PAAm, PVP and PAA nanogels. These data can be referred that some of acrylamide groups of these nanogels can be hydrolyzed to carboxylic groups at pH 10 and generates negative charges which repulse with negative charges of clay layer that decreased the Na-MMT contents in these nanogels [41].

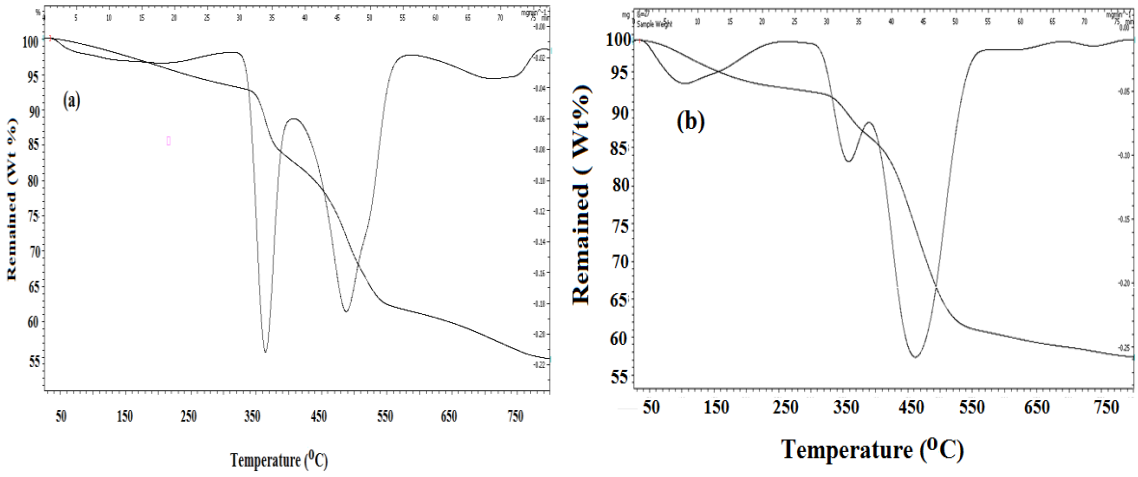

Fig.2. TGA and DTG thermograms of a) Na-MMT/PAMPS-Na snd b) Na-MMT/PAMPS nanogels

Table1. TGA data of amphiphilic Na-MMT nanogels and percentages of crosslinking polymerization

Na-MMT Nanogels modifier	Remaining		Actual amounts relate to Na-MMT (Wt%)	Crosslinking copolymerization %
	Temperature range (^{o}C)	Weight loss (%)		
PAMPS-Na	50-350	8	45	96.1
	350-650	37		
	Residue at 650 ^{o}C	55		
PAMPS	50-300	30	35	90.32
	300-650	35		
	Residue at 650 ^{o}C	55		
PVP	50-350	8	50	96.8
	350-650	40		
	Residue at 650 ^{o}C	52		
PNIPAm	50-275	8	42	95.2
	350-650	52		
	Residue at 650 ^{o}C	40		
PAAm	50-300	11	46	85.42
	300-650	44		
	Residue at 650 ^{o}C	46		
PAA	50-300	18	40	80.23
	300-650	44		
	Residue at 650 ^{o}C	38		

On the other hand, the Na-MMT coated with either PAMPS or PAMPS-Na showed more Na-MMT contents than other nanogels. This behavior can be referred to the stability of amide groups of PAMPS or PAMPS-Na to hydrolysis and to increased their ability of amide to produce questionable zwitterionic form that increased the interaction between Na-MMT clay galleries and AMPS, as claimed by Xu et al. [40].

The morphology of Na-MMT nanogels can be represented from TEM photos (Fig. 3). TEM photos are the best proof for success or failure, coating or encapsulation of Na-MMT sheets. TEM image of Na-MMT (Fig.3 a) reveals that the Na-MMT has a compact sheets. The TEM images of Na-MMT nanogels (Fig. 3 b-h) showed different morphologies as uncoated Na-MMT sheets, Na-MMT nanogels core shell structure with will defined morphology and separated spherical nanogels. The Na-MMT galleries were completely surround by the PAMPS, PAMPS-Na and PNIPAm nanogels (Fig. 3b-d). The Na-MMT/PAAm nanogel (Fig.3e) showed uncoated Na-MMt and separated spherical PAAm nanogels. Na-MMET/PAA and NAMMT/PVP showed agglomerates morphologies [Fig. 3f a- g]. From the dispersant-limited agglomeration theory [42], it is well known that the formation of unstable polymer particles produced polymer agglomerates. The presence of PVP stabilizers that have not insufficient ability to cover the total surface area of the nanogel particles, redistributes onto the reduced surface area of the aggregates and prevents further agglomeration. In our system, this process could occur with the nanogels that cannot coat or interact with Na-MMT galleries due to repulsive forces between negative charges of nanogel particles such as carboxylate ions of PAA and negative charges of Si-O^{-} of Na-MMT sheets. Moreover, The presence of crosslinked PVP nanogels (Fig.3 g) produced Na-MMT agglomerates. As reported by Haraguchi et al.[43], it can be proposed that the initiated monomers formed reactive polymer chain at the surface of clay platelets through polar interactions to produce ‘‘clay-brush particles’’. These brushes are composed of exfoliated clay platelets and number of grafted chains [**39**]. Wide-angle XRD (WXRD) analysis is an useful technique used to determine the

intercalation, exfoliation of that clay platelets that can act as a kind of physical multifunctional cross-linker to prepare micro and nano-gels [39]. In this respect, WXRD diffractograms of Na-MMT nanogels are represented in Fig.4. It was noticed that, Na-MMT showed strong diffraction peak at around 6.214^{o}, corresponding to a d- basal spacing of (001) layer is 1.486 nm (Fig. 4 a). The position of this peak was changed to 2.74 and 7.9^{o} and basal spacing of these peak are 2.871 and 4.953 nm for Na-MMT crosslinked with PAMPS-Na and PAMPS nanogels, respectively (Fig. 4 c and d). The increment of d- basal spacing of the silicate layers indicates the intercalation of Na-MMT with PAMPS and PAMPS-Na nanogels[44]. Moreover, the differences in the position of 001 peak and d-spacing indicated that

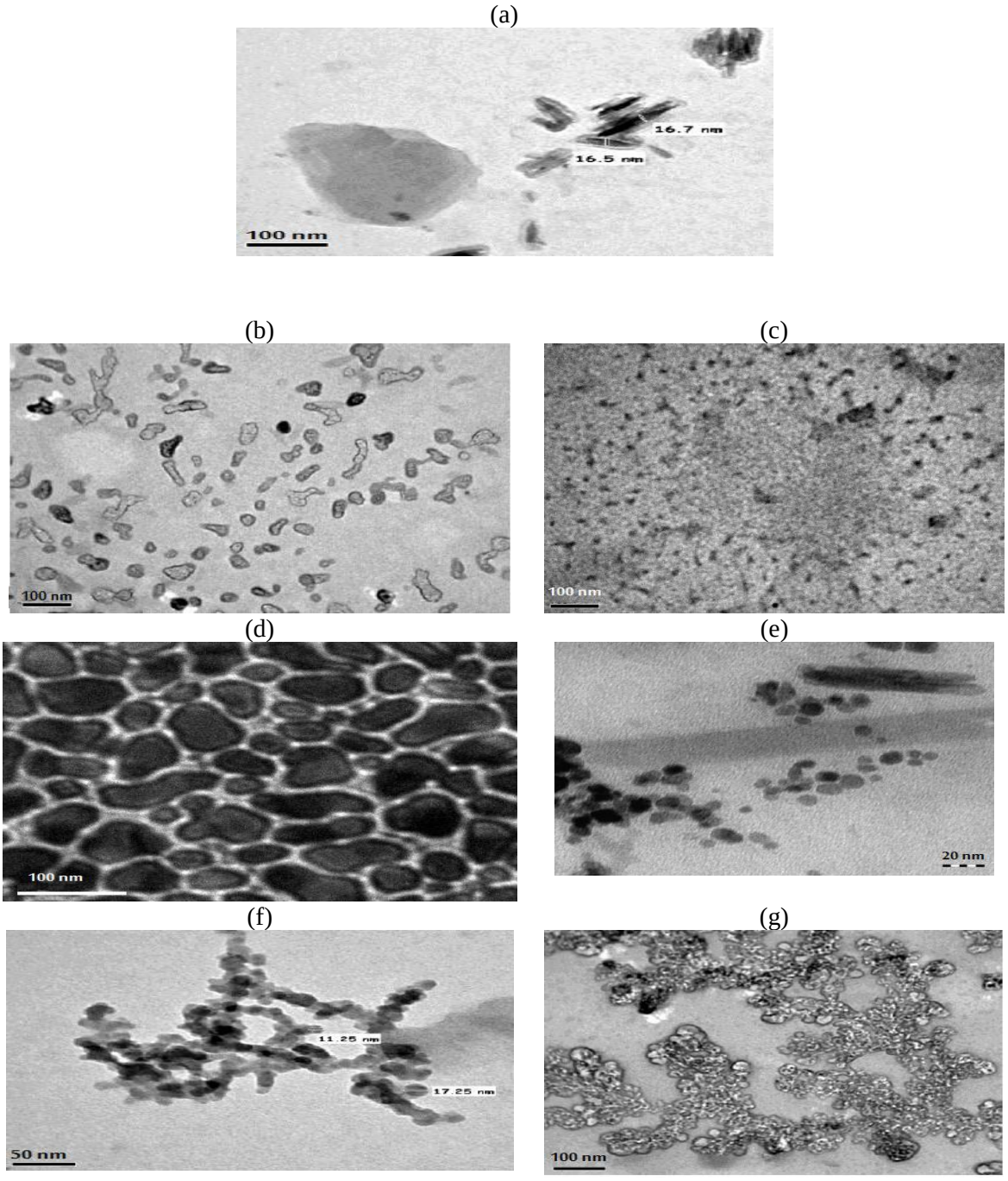

Fig.3. TEM photos of a) Na-MMT, b) Na-MMT/PAMPS, c) Na-MMT/PAMPS-Na, d) Na-MMT/NIPAm, e) Na-MMT/PAAm, f) Na-MMT/PAA and g) Na-MMT/PVP nanogels.

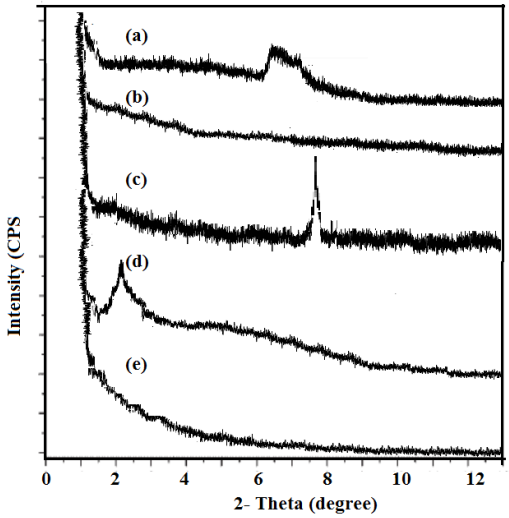

Fig. 4. WXRD diffractograms of a) Na-MMT, b) Na-MMT/PNIPAm , c) Na-MMT/PAMPS, d) Na-MMT/PAMPS-Na and e) Na-MMT/PVP nanogels

PAMPS and PAMPS-Na interacted and arranged with the silicate layer with different arrangements [45]. Fig, 4 b and e shows that no distinct diffraction peak is observed in a range from 1.5 to 14^{o} for Na-MMT crosslinked with PVP and PNIPAm nanogels. Therefore, it can be concluded that Na-MMT platelets are present at an exfoliated state when crosslinked with nonionic PNIPAm and PVP nanogels. This result confirm that the diffusion of NIPAm and VP between silicate layer can be easily obtained due to the polar interactions between amide groups of monomers and silicate layer that facilitates the exfoliation of silicate layers. The presence of hydrophobic isopropyl and cyclopentane groups and absence of anions such as sulfonate (PAMPS and PAMPS-Na) or carboxylate (PAA)) increased the arrangements of PNIPAm and PVP nanogels between silicate layers. WXRD data of Na-MMT crosslinked with PAAm and PAA (were not included for brevity) showed no change in the position of peak at 5.988^{o} that indicated PAA and PAAm nanogels are not effectively to exfoliate or intercalate the Na-MMT layers.

3.2. Surface properties of Na-MMT nanogels

It is important to study the surface and interfacial properties of amphiphilic particles, especially nanoparticles, due to their superior properties [46-48]. The commercially available nanoparticles are mostly not surface active due to their either extreme hydrophilicity or hydrophobicity [10]. In the present work, the interaction of the clay solid particles with amphiphile nanogels has been developed

to modify the surface activity or wettability of the particles. Using this technique, the surface activity of the clay solid particles can be controlled by selection of the most favorable molecular structure of the amphiphile nanogels. Accordingly, the interaction between amphiphile nanoparticles and water has become a fascinating subject. In this respect, the relation between the equilibrium dynamic surface tension of amphiphilic nanoparticles and their concentration can be used to investigate the surface activity of these particles. It is necessary in this work to confirm that there uncrosslinked polymers and monomers were removed during purification of Na-MMT nanogels as described in the experimental section. The surface tension (γ) of the supernatant removed from the last method of purification is 74.3 mN/m that concluded that the surface tension of the purified dispersed Na-MMT nanogels does not contain impurity. The relation between γ of Na-MMT nanogels and their concentrations - ln (C; mol/L) was represented in Fig. 5. The critical aggregation concentrations (cac; mol/L) of Na-MMT nanogels can be determined from Fig. 5 at the concentrations that the surface tension of the dispersed Na-MMT nanogels started to sharply increase. The surface tension at this concentration knows as γ_{cac}. The cac and γ_{cac} were determined from Fig. 5 and listed in Table 2. The cac data indicated that the Na-MMT

nanogels form aggregates in the bulk water solution can be arranged in the order PVP>PAAm>PAMPS> PNIPAm>PAMPS-Na nanogels. That means that the dispersability of Na-MMT nanogels in water can be arranged in the reverse order. It can be also measured the effectiveness of the Na-MMT nanogels (π_{cac}; mN/m) to reduce the surface tension of water from equation; $\pi_{cac} = \gamma_o - \gamma_{cac}$, where γ_o is surface tension of pure water at 25 ^oC (72.1 mN/m). The π_{cac} values were calculated and listed in Table 2. The data indicated that the efficiency of Na-MMT nanogels to reduce surface tension of water can be arranged in the order PNIPAm> PVP> PAMPS-Na >PAMPS> PAAm. This confirms that the presence of hydrophobic groups such as isopropyl, methylpropyl, cyclopentane increased the amphiphilic character of Na-MMT nanogels due to the hydrophilic and hydrophobic interactions balance between Na-MMT nanogels and water.

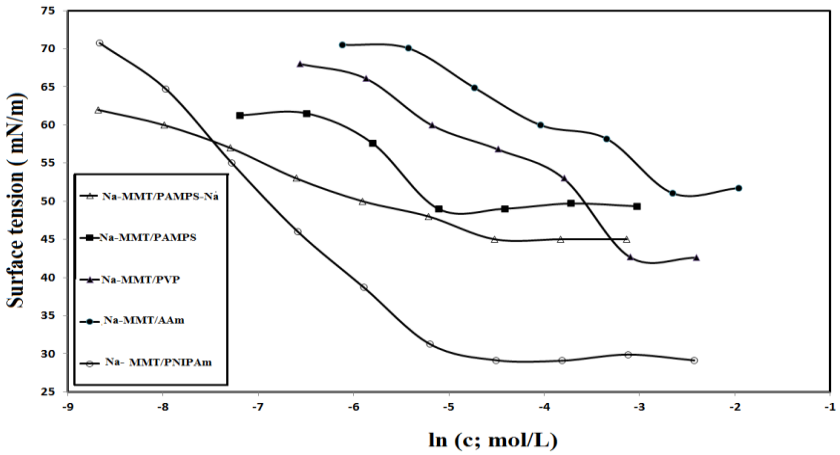

Fig. 5. Relations between equilibrium surface tension of Na-MMT nanogels and their different concentrations at 25 ^oC.

Table 2. Surface activity parameters of amphiphilic Na-MMT nanogels in water at 25 ^oC.

Na-MMT Nanogels modifier	cmc mol/L x 10^3	γ_{cmc} mN/m	$\Delta\gamma = \gamma_{o-} \gamma_{\pi cmc}$ mN/m	$(-\partial \gamma / \partial \ln c)$	Γ_{max} x 10^{10} mol/ cm^2	A_{min} nm^2/ molecule
PNIPAm	5.6	29.2	42.0	10.23	6.45	0.258
PAMPS-Na	9.1	45.1	27.0	7.5	3.15	0.527
PAMPS	4.1	50.1	22.0	4.25	1.78	0.932
PVP	0.35	42.7	29.4	6.97	2.92	0.569
PAAm	0.52	53.3	18.8	5.68	2.38	0.698

It was also concluded that the repulsion between sulfonate groups of Na-MMT/PAMPS-Na nanogels decreases the formation of aggregates and increases the possibility to reduce the surface tension of water more than its nonionized form of Na-MMT/PAMPS.

The surface activity of Na-MMT nanogels can be investigated by measuring the concentrations of Na-MMT nanogels at air/water interface as determined from surface excess concentration (Γ_{max}) that was calculated from the equation:

$$\Gamma_{max} = 1/RT \text{ x } (-\partial\gamma / \partial \ln c)_T, \text{ where } (-\partial\gamma / \partial \ln c)_T \qquad (3)$$

The equation is the slope of the plot of γ versus ln c at constant temperature (T) and R is the gas constant (in J/mol.K). The Γ_{max} values were used to determine the minimum area A_{min} at the air/water interface that provides information on the degree of packing and the orientation of

the adsorbed Na-MMT nanogels, when compared to the dimensions of the molecule obtained from models. A_{min} is calculated using the equation:

$$A_{min} = 10^{16} / N \Gamma_{max} \quad (4)$$

Where N is Avogadro's number, and the data for Γ_{max}, A_{min}, and $(-\partial\gamma / \partial \ln c)$ were determined and listed in Table 2. The data indicated that the ability of Na-MMT nanogels to be efficiently adsorbed at air/water interface can be arranged in the order PNIPAm>PAMPS-Na>PVP>PAAm>PAMPS nanogels. The amphiphilic characters of Na-MMT nanogels in water encouraged us to apply these amphiphiles to remove pollutants from water.

3.3. Application of Na-MMT nanogels for water treatments:

It was reported that, the low cost and environmentally friendly adsorbents attracted great attention for removal of toxic materials such as dyes and toxic heavy metals from industrial water [**49**]. Clay minerals among several types of natural and synthetic adsorbents have been widely used for industrial water treatments due to their natural availability, high adsorption capacity for cations and polar molecules, recyclability, low cost and their nontoxic effects on the environment[**50].** The present work aims to modify the chemical structure of Na-MMT by nanogels to increase its adsorption rate of pollutant removal, selectivity and recyclability. In this respect, the modified Na-MMT nanogels are used to remove organic and inorganic pollutants from water. MB as cationic dye is selected as organic substance. Ni^{2+} and Co^{2+} cations are selected as inorganic pollutants. The removal efficiency (% E) and the amounts of adsorbate (mg/g) at equilibrium (qe) of Na-MMT nanogels are used to evaluate their capability to remove organic and inorganic pollutants (as described in the experimental section). The effects of pH and contact time on q_e are evaluated to predict the mechanism of adsorption.

The initial pH values of the water pollutants are very important parameter that affect the adsorption capacities of the polar adsorbents [51]. The relation between initial pH value of dispersed Na-MMT solution (at 1000 ppm) and their q_e values (mg/g) for MB, Ni and Co cations was illustrated in Fig.6a-c, respectively. The ionic strengths of solution were kept at 0.1M. The data confirmed that all Na-MMT nanogels showed low q_e value in lower acidic pH value. This can be referred to protonation of amide groups of Na-MMT nanogels which repulse with positive charges of MB, Co and Ni cations and reduce the uptake of Na-MMT nanogels.

Table 3. The DLS and Zeta Potential measurements of the Na-MMT nanogels.

Na-MMT nanogels	DLS		Zeta Potential (mV)		
	Particle size(nm)	PDI	pH 4	pH 7	pH 9
Na-MMT	30 ± 12	1.23	-18.10	-22.44	-30.50
PNIPAm	45 ± 10	0.856	-10.2	-50.13	-55.41
PAMPS-Na	40± 8	0.478	-26.4	-30.2	-48.3
PAMPS	50± 5	0.359	-8.3	-25.8	-40.3
PVP	60± 20	1.56	-20.4	-38.2	-45.3
PAAm	100± 50	1.892	-25.3	-40.2	-48.2
PAA	40± 10	0.968	-10.3	-28.1	-33.2

The all measurements were carried out in 10^{-3} M KCl

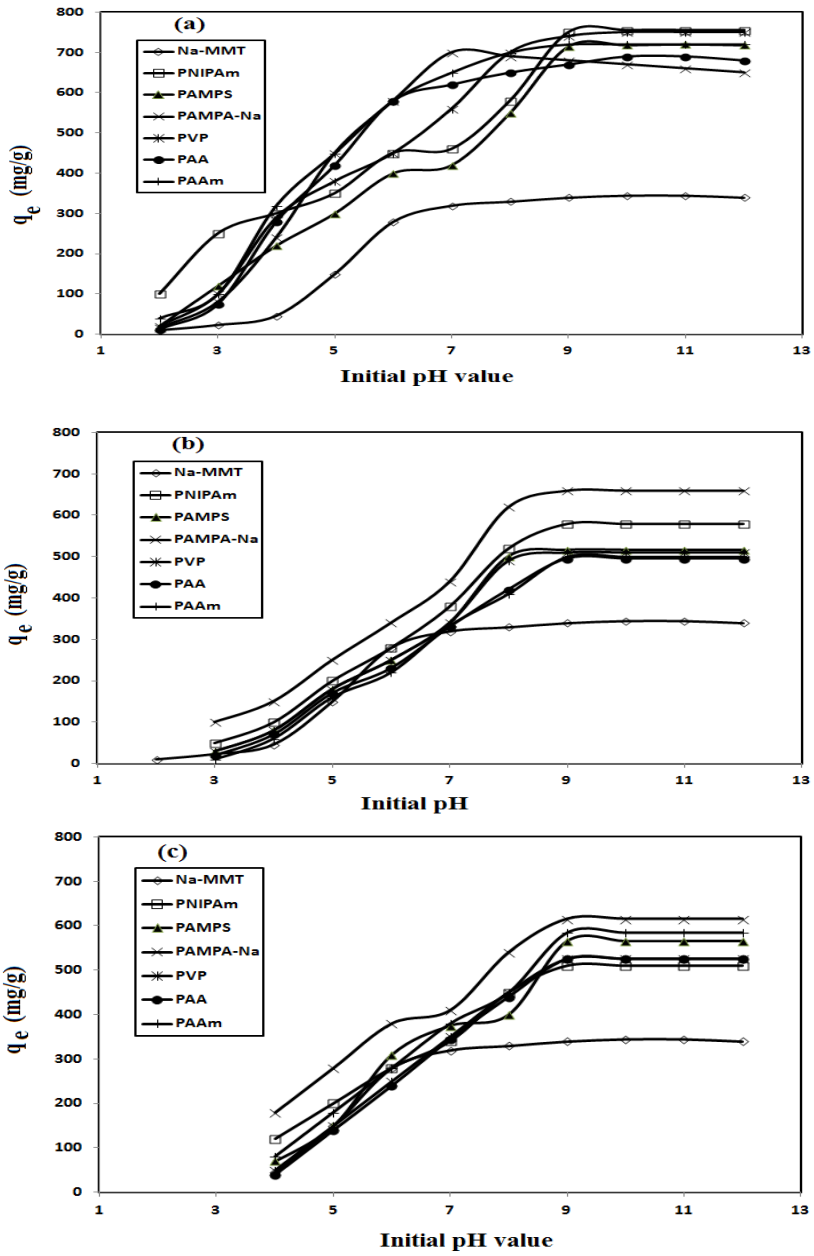

Fig.6. Relation between equilibrium adsorption capacities of Na-MMT nanogels at 1000 ppm in their initial pH of a) MB, b) Co^{2+} and c) Ni^{2+} aqueous solution at 25 ^{o}C.

It was also observed that the q_e increased with increasing pH value up to 9 and 7 for removal of MB and Co or Ni cations. Further increasing in the pH did not affect any significant changes except Na-MMT/PAMPS-Na due to deshielding effect of more Na cations that screen the sulfonate ionic networks. The effect of pH of solutions on the zeta potential (ζ; mV) of Na-MMT solution was determined using DLS measurements in the presence of 0.001M of KCl. The particle size, polydispersity index (PDI) and ζ values of Na-MMT at different pH solutions were determined and listed in Table 3. It was noticed that ζ values are negative at different pH for all modified Na-MMT nanogels and more negative value than that unmodified Na-MMT. This was refereed to formation of hydrogen bonds between amide groups of nanogels and hydroxylated silicates in montmorillonite that increases the zeta potential of silica and alumina edges [52-53].

Effect of pollutant concentrations on the removal efficiencies (%E) is very important parameters that can be used to correlate the adsorbent chemical structure with its removal efficiency. Therefore, the relation between removal efficiency of MB dye of Na-MMT nanogels and its

concentration in aqueous solution of pH 9, ionoic strength 0.1M at 25 ^{o}C was determined and illustrated in Fig.7 as representative.

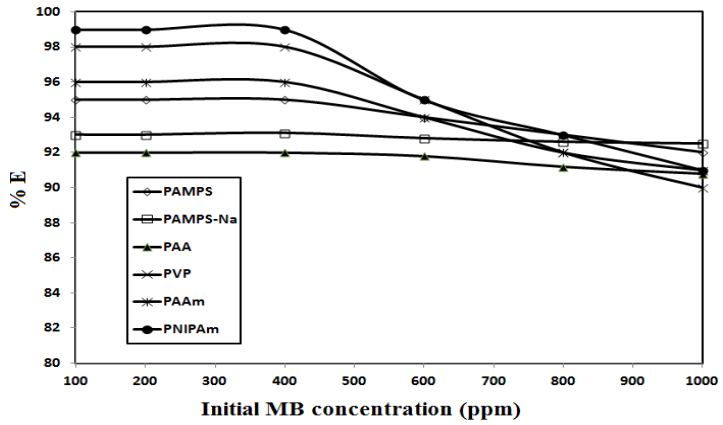

Fig.7. Relation between MB removal efficiencies of Na-MMT nanogels and their different concentrations in aqueous solution at 25 ^{o}C

Careful inspection of data indicated that the MB removal efficiencies of Na-MMT nanogel can be arranged in the order of PNIPAm> PVP> PAAm > PAMPS-Na> > PAMPS>PAA that resemble to ability of nanogels to reduce water surface tension as represented in previous section. While the %E of metal cations can be arranged in the order PNIPAm>PAMPS-Na>PVP>PAAm>PAMPS which agree with the order of nanogels to adsorb at interfaces. This means that the ability of Na-MMT nanogels to reduce the surface tension of water facilitate the diffusion of organic dye (MB) into the network structure of nanogels. Moreover, the confirmation and assembly of Na-MMT nanogels at interfaces affect the interactions between metal cations and active polar sites of nanogels. Therefore, the larger vacant available active site of Na-MMT nanogels are responsible for the total removal of inorganic pollutants that increased at lower Na-MMT concentrations [**54].**

One of the interesting characteristics of Na-MMT is attributed to its ability to remove the pollutants in short time ranged from 20 to 40 minutes that was not reported before for clay minerals. In this respect, the equilibrium times for removal 1000 ppm of MB are 20, 25, 30, 35, 40, 45 and 180 minutes for Na-MMT/PNIPAm, PVP, PAAm, PAMPS-Na, PAMPS and Na-MMT. The data indicated that, more than 60 % of MB is removed during 5 to 15 minutes based on the nanogel types. This was referred to an increase in mass transfer driving force and the resultant increase in MB adsorption. Moreover, that could also related to an

increase the number of reactive vacant sites available early on. However, the number of these sites reduced with time due to accumulation of dye on these sites that affects the adsorption rate of Na-MMT until reached they reached the adsorption equilibrium.

3.4. Adsorption isotherms

The Langmuir and Freundlich models are the most important among different models that used to describe the experimental data of adsorption isotherms. The experimental data confirmed Langmuir model confirm the maximum adsorption of adsorbate molecules is referred to the formation of homogeneous saturated monolayer of adsorbate at the adsorbent surfaces. Moreover, the energy of adsorption is constant without metempsychosis of adsorbate molecules. The Freundlich isotherm confirms that the adsorption of adsorbate molecules take place at heterogeneous surfaces of adsorbents. the Langmuir isotherm equation (5), [**55**] or Freundlich equation (6) [**56**] to describe the homogeneity and heterogeneity of the adsorption behaviors:

$$(C_e/Q_e) = [(1/Q_{max}\, K_l) + (C_e/ Q_{max})] \quad (5)$$

$$\log (Q_e) = \log (K_f) + [(1/n) \times \log (C_e)] \quad (6)$$

Where Q_e and Q_{max} are the equilibrium and maximum amount of dye (mg/g) adsorbed on Na-MMT nanogel composites. C_e is the concentration of dye solution at equilibrium (mg/L). The K_l and K_f are Langmuir and Freundlich constants that determined from relation of C_e/Q_e against C_e and ln Q_e as the function of ln C_e, respectively at 25 ^oC as presented in (Fig. 8).

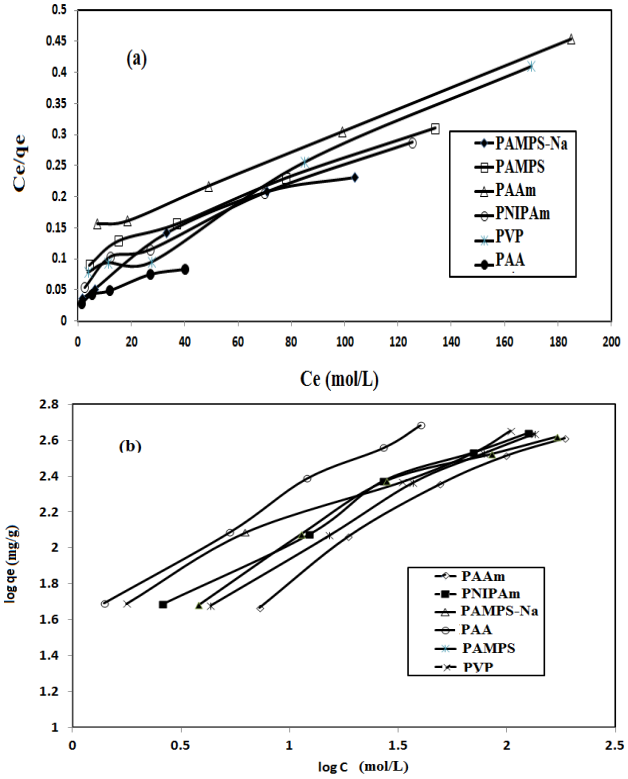

Fig.8. Adsorption isotherms a)Langmuir and b) Freundlich models of Na-MMT nanogels

The K_l and K_f values [L/mg] are used to represent the interaction energy between the adsorbate and the adsorption sites of Na-MMT nanogels. The n value is the adsorption intensity and their values indicated the favorable ability of the adsorption process. The values of $0< 1/n< 1$, that determined as slop of equation (6) represent favorable adsorption conditions [57]. The Langmuir and Freundlich model parameters correlate with the experimental data Q_{max} and % E and listed in Table 4.

Table 4. Adsorption isotherm parameters for removal of 1000 ppm of MB dye using amphiphilic Na-MMT nanogels at 25 ^{o}C

Adsorbents	Langmuir isotherm parameters			Freundlich parameters			Exp. Adsorption capacity
	Q_{max} mg/g	K_l L/mg	R^2	1/n	K_f	R^2	Q_{max} (mg/g)
Na-MMT	344.3	0.0271	0.9817	0.6863	0.049	0.906	310
Na-MMT/PNIPAm	625.1	0.0245	0.9933	0.2369	0.190	0.8402	600
Na-MMT/ PAAm	714	0.0103	0.998	0.699	0.064	0.937	720
Na-MMT/PAA	620	0.0501	0.953	0.681	0.205	0.995	670
Na-MMT/PAMPS-Na	600	0.0341	0.997	0.513	0.205	0.986	680
Na-MMT/PAMPS	700	0.0151	0.99	0.650	0.111	0.99	715
Na-MMT/PVP	714	0.0221	0.997	0.599	0.158	0.9935	745

The best equilibrium model was selected based on the linear square regression correlation coefficient, R^2 (Table 4). The measured data for the adsorption of MB follow Langmuir model and achieved good regression coefficients R^2 than that of the Freundlich model except that Na-MMT/PAA nanogel. Moreover, it was noticed that the Q_{max} values for the adsorption of MB onto the Na-MMT nanogels calculated from the Langmuir model are all the same as the experimental data (Table 4). These data confirm that all of the Na-MMT nanogel adsorption sites have equal adsorbing affinities. The lower value of 1/n below 1 indicates that the Na-MMT surfaces have sufficient enough area for MB adsorption separation.

4. Conclusions

In summary, a facile route to prepare colloidal Na-MMT homopolymer nanogels via the free radical polymerization of vinyl monomers in the presence of an dispersed Na-MMT mineral is reported. We concluded that this approach represents a new paradigm in the synthesis of amphiphilic clay mineral via "surfactant-free" nanogel colloids. The resulting nanogel composite particles have relatively narrow and wide size distributions, mean particle diameters of 30-80 nm and Na-MMT contents of 40-54%. TEM micrographs confirm a "currant-bun" particle morphology, in which most of the Na-MMT particles are encapsulated within the homopolymer nanogels. The adsorption data indicated that the MB removal efficiencies of Na-MMT nanogel can be arranged in the order of PNIPAm> PVP> PAAm > PAMPS-Na> > PAMPS>PAA that resemble to ability of nanogels to reduce water surface tension. While the %E of metal cations can be arranged in the order PNIPAm>PAMPS-Na>PVP>PAAm>PAMPS that agree with the order of nanogels to adsorb at interfaces. This confirms that the ability of Na-MMT nanogels to reduce the surface tension of water facilitate the diffusion of organic dye (MB) into the network structure of nanogels. Moreover, the confirmation and assembly of Na-MMT nanogels at interfaces affect the interactions between metal cations and active polar sites of nanogels.

Acknowledgment

The project was financially supported by King Saud University, Vice Deanship of Research Chairs.

References

[1] C. H. Zhou, J.Keeling, Applied Clay Science, **74**, 3-9 (2013).
[2] N. An, C. H. Zhou, X. Y. Zhuang, D. S. Tong, W. H. Yu Applied Clay Science, **114**, 283 (2015).
[3] G.D. Yuan, B.K.G. Theng, G.J. Churchman, W.P. Gates, in developments in Clay Science, "Clays and Clay Minerals for Pollution Control", F. Bergaya and G. Lagaly, Elsevier Ltd. Oxford OX5 1GB, UK, **5**, 587 (2013).
[4] J. M. Gatica, H. Vidal, Journal of Hazardous Materials, **181**, 9 (2010).
[5] E.G. Garrido-Ramírez, B.K.G. Theng, M.L. Mora, Applied Clay Science, **47**, 182 (2010).
[6] S. S. Ray, in Clay-containing Polymer Nanocomposites, "An Overview of Pure and Organically Modified Clays", Elsevier Ltd. Oxford OX5 1GB, UK, pp1-24 (2013).
[7] D. Songurtekin, E. E. Yalcinkaya, D. Ag, M. Seleci, D. O. Demirkol, S. Timur, Applied Clay Science, **86**, 64 (2013).
[8] M. G. M. Nguemtchouin, M. B. Ngassoum, R. Kamga, S. Deabate, S. Lagerge, E. Gastaldi, P. Chalier, M. Cretin, Applied Clay Science, **104**, 110 (2015).
[9] G. Choudalakis, A.D. Gotsis, European Polymer Journal, **45**, 967 (2009).
[10] Emmanuel I. Unuabonah, Andreas Taubert, Applied Clay Science, **99,** 83 (2014).
[11] B. F. Urbano, B. L. Rivas, F. Martinez, S. D. Alexandratos, Reactive and Functional Polymers, **72**, 642 (2012).
[12] J. Faucheua, C. Gauthiera, L. Chazeaua, J.Y. Cavailléa, V. Mellonb, E. B. Lami, Polymer, **51**, 6 (2010).
[13] K. M. Ardakani, B. Nazari, Composites Science and Technology, **70**, 1557 (2010).
[14] B. Chen, J. R.G. Evans, Polymer, **49**, 5113 (2008).
[15] A. Pegoretti, A. Dorigato, M. Brugnara, European Polymer Journal, **44**, 1662 (2008).
[16] S. Maisanaba, S. Pichardo, M. Puerto, D. Gutiérrez-Praena, A. M. Cameán, A. Jos, Environmental Research, **138**, 233 (2015).
[17] A. Contin, A. Biffis, S. Sterchele, K. Dörmbach, S. Schipmann, A. Pich, Journal of Colloid and Interface Science, **414**, 41 (2014).
[18] C. Buratti, E. Moretti, in Nanotechnology in Eco-Efficient Construction, "Silica nanogel for energy-efficient windows", Elsevier Ltd. Oxford OX5 1GB, UK, 207-235 (2013).
[19] M. Motornov, Y. Roiter, I. Tokarev, S. Minko, Progress in Polymer Science, **35**, 174 (2010).
[20] M. M. Yallapu, M. Jaggi, S. C. Chauhan, Drug Discovery Today, **16**, 457 (2011).
[21] L. L Beecroft, C. K. Ober, Chem. Mater. **9**, 1302 (1997).
[22] K. K. W. Wong, T. Douglas, S. Gider, D. D. Awschalom, S. Mann, Chem. Mater. **10**, 279 (1998).
[23] K. K. W Wong, S. Mann, Adv. Mater. **8**, 928 (1996).
[24] M. A. Akl, A. M. Atta, A. M. Yousef, M.I. Alaa, Polymer International, **62**, 1667 (2013).
[25] M. J. Percy, C. Barthet, J. C. Lobb, M. A. Khan, S. F. Lascelles, M. Vamvakaki, S. P. Armes, Langmuir **16**, 6913 (2000).
[26] S. Fujii, S. P. Armes, B. P. Binks, R. Murakami, Langmuir, **22**, 6818(2006)..
[27] F. Tiarks, K. Landfester, M. Antonietti, Langmuir **17**, 5775 (2001).
[28] D. Dupin, A. Schmid, J. A. Balmer, S. P. Armes, Langmuir **23**, 11812 (2007).
[29] A. Schmid and P. A. Steven, Langmuir **25**, 2486 (2009).
[30] A. Slistan-Grijalva, R. Herrera-Urbina, J. F. Rivas-Silva, M. Avalos-Borja, F. F. Castill´on-Barraza, A. Posada-Amarillas, Materials Research Bulletin, **43**, 90 (2008).
[31] R. Levy and C. W. Francis, Journal of Colloid And Interface Science, **50**, 442 (1975).
[32] A. E. Blum and D. D. Eberl, Clays and Clay Minerals, **52**, 589 (2004).
[33] K. A. Carrado, L. Xu, Microporous and Mesoporous Materials, **27**, 87(1999).
[34] N. Jovic-Jovicic, A. Milutinovic-Nikolic, P. Bankovic, Z. Mojovic, M. Zunic, I. Grzetic, D. Jovanovic, Applied Clay Science, **47**, 452 (2010).
[35] S.M. Lee, Tiwari D. Applied Clay Science, **59-60**, 84 (2012).
[36] S. S. Ray, M. Okamoto, Prog. Polym. Sci. **28**, 1539 (2003).

[37] F. Bergaya, G. Lagaly, Appl. Clay Sci. **19**, 1 (2001).
[38] A. M. Atta, G. A. El-Mahdy, H. A. Al-Lohedan, A. M. Tawfeek, S. R. Sayed, Int. J. Electrochem. Sci., **10**, 2377 (2015).
[39] Q. Zhang, L. Zha, J. Ma, B. Liang, Macromol. Rapid Commun. **28**,116 (2007).
[40] M. Xu, Y.S. Choi, Y.K. Kim, K.H. Wang, I. J. Chung, Polymer **44**, 6387 (2003).
[41] Y. Deng, J.B. Dixon, G.N. White, Soil Sci. Soc. **70**, 297 (2006).
[42] A. J. Paine, Macromolecules, **23**, 3109 (1990).
[43] K. Haraguchi, H. J. Li, K. Matsuda, S. Okabe, T. Takehisa, E. Elliot, Macromolecules, **38**, 3482 (2005).
[44] A. M. Atta, G. A. El-Mahdy, H. A. Al-Lohedan, A. M. Tawfeek, A. A. Abdel-Khalek, Digest Journal of Nanomaterials and Biostructures **9**, 531 (2014).
[45] Z. Hu, G. He, Y. Liu, C. Dong, X. Wu, W. Zhao, Applied Clay Science, **75-76**,134 (2013).
[46] S. Tcholakova, N. D. Denkov, A. Lips, Phys. Chem. Chem. Phys. **10**, 1608 (2008).
[47] T. N. Hunter, R. J. Pugh, G.V. Franks, G. J. Jameson, Adv. Colloid Interface Sci. **137**, 57 (2008).
[48] A. Böker, J. He, T. Emrick, T.P. Soft Matter **3**, 1231 (2007).
[49] R. Aveyard, B.P. Binks, J.H. Clint, Adv. Colloid Interface Sci. **100–102**, 503 (2003).
[50] S. M. Lee, D. Tiwari, Applied Clay Science, **59–60**, 84 (2012).
[51] L. Hem, V. K. Garg, , R. K. Gupta, Dyes Pigments **74**, 653 (2007).
[52] S.F. Wang, L. Shen, Y.J. Tong, L. Chen, I.Y. Phang, P.Q. Lim, T. X. Li, Polymer Degradation and Stability **90**, 123(2005).
[53] I. Sondi, O. Milat, V. Pravdic, J. Colloid Interface Sci. **189**, 66 (1997).
[54] V.S. Mane, I.D. Mall, V.C. Srivastava, J. Environ. Manag. **84**, 390 (2007).
[55] I. Langmuir, J. Am. Chem. Soc. **38**, 2221 (1916).
[56] U. Freundlich, J. Phys. Chem. **57**, 385 (1906).
[57] G.F. Cerofolini, M. Jaroniec, S. Sokosvski, Colloid Polym. Sci. **256**, 471 (1978).